

See discussions, stats, and author profiles for this publication at: <https://www.researchgate.net/publication/263355178>

# Intramolecular Cycloadditions of Photogenerated Azaxylylenes: An Experimental and Theoretical Study

ARTICLE *in* THE JOURNAL OF PHYSICAL CHEMISTRY A · JUNE 2014

Impact Factor: 2.69 · DOI: 10.1021/jp504281y · Source: PubMed

---

CITATIONS

2

---

READS

17

## 6 AUTHORS, INCLUDING:



N. N. Kumar

University of Denver

24 PUBLICATIONS 670 CITATIONS

[SEE PROFILE](#)



chandra sekhar

University of Hyderabad

4 PUBLICATIONS 24 CITATIONS

[SEE PROFILE](#)

# Intramolecular Cycloadditions of Photogenerated Azaxylylenes: An Experimental and Theoretical Study

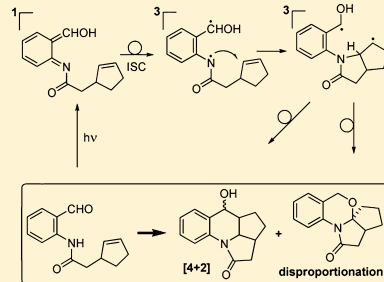
Olga A. Mukhina,<sup>†,‡</sup> W. Cole Cronk,<sup>†,‡</sup> N. N. Bhuvan Kumar,<sup>†</sup> M. Chandra Sekhar,<sup>§</sup> Anunay Samanta,<sup>§</sup> and Andrei G. Kutateladze\*,<sup>†</sup>

<sup>†</sup>Department of Chemistry and Biochemistry, University of Denver, Denver, Colorado 80208, United States

<sup>‡</sup>School of Chemistry, University of Hyderabad, Hyderabad, India 500046

## Supporting Information

**ABSTRACT:** The mechanism of intramolecular cycloadditions of azaxylylenes photogenerated via excited-state intramolecular proton transfer (ESIPT) in aromatic *o*-amido ketones and aldehydes bearing unsaturated functionalities was studied experimentally and computationally. In time-correlated single-photon counting experiments, no relation was found between lifetimes of singlet species and the nature of the amide pendant, either unsaturated furanpropanamide, capable of photocyclization, or the acetamide control. Steady-state emission for amido-tetralone derivatives showed comparable dual emission bands, but bromo substitution decreased the intensity of the ESIPT band. The most reactive derivatives of amidobenzaldehydes were virtually lacking the ESIPT band. The quantum yield of cycloaddition is decreased in the presence of triplet quenchers, O<sub>2</sub> or *trans*-piperylene, and improved with heavy atom substitution in the aromatic ring, providing further evidence for the initial mechanistic hypothesis in which the fast singlet-state ESIPT is accompanied by the ISC in the tautomer (azaxylylene), which undergoes stepwise addition to the tethered unsaturated pendants.



## 1. INTRODUCTION

Derivatives of aromatic *ortho*-aminoketones or aldehydes undergo fast excited-state intramolecular proton transfer (ESIPT) producing intriguing tautomeric intermediates, C-hydroxyazaxylylenes, Figure 1.

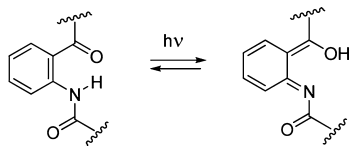


Figure 1. ESIPT producing azaxylylenes in aromatic *o*-amidoketones.

The photophysics of these processes was studied extensively using primarily derivatives of aminoanthraquinone as it offers convenience of strong transient absorption and dual emission from the two tautomers. Both singlet<sup>1–3</sup> and triplet-state<sup>4–7</sup> photophysics of aminoanthraquinones was addressed in the early studies. In 1991, Smith and Barbara gave a comprehensive account of these processes.<sup>8</sup> They found that for 1-acylaminoanthraquinones, the long-wavelength emission and short-wavelength emission are both established within 300 fs. One of the important conclusions of their study is that while ESIPT is extremely rapid, it is not always the dominant process. For weakly acidic amides, intersystem crossing (ISC) from the S<sub>1</sub> state of the original amide is important. Another conclusion was that the asymmetry of the potential energy surface (PES) of the singlet excited state can be controlled by substitution, allowing for 2 orders of magnitude variations in the dual

emission ratio. Solvent effects on observed lifetimes and fluorescence efficiency<sup>8</sup> and also on the rate of ISC and triplet yields<sup>7</sup> were found to be very important. In 2005, Blank<sup>9</sup> and co-workers published a very sophisticated work on the dynamics of intermolecular solvent response affecting these intramolecular proton-transfer processes.

With all of this wealth of photophysical observations now available it is curious that unlike their all-carbon cousins, xylylenes,<sup>10–20</sup> azaxylylenes photogenerated via ESIPT were not employed in cycloaddition reactions until our work on their intramolecular trapping, which offered an expedited approach to a variety of polyheterocyclic scaffolds of great practical interest.<sup>21–24</sup> A typical reaction is shown in Figure 2. Both [4 + 4] and [4 + 2] photocyclization products could be formed. In order to take advantage of everything that this synthetic

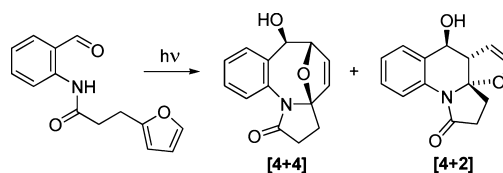


Figure 2. Photoinduced cyclization in furanpropanamide of amino-benzaldehyde.

## Special Issue: Current Topics in Photochemistry

Received: May 1, 2014

Revised: June 5, 2014

Published: June 24, 2014



methodology can offer, it is critical to understand the underlying photophysics and photochemistry. In this paper, we report our experimental and theoretical mechanistic study of the intramolecular cycloadditions of photogenerated hydroxylazaylylenes.

## 2. METHODS

Compounds **1–13** were synthesized according to the methods described previously.<sup>21,24</sup> Synthesis of **14** and **15** is described in the Supporting Information. NMR spectra were recorded at 25 °C on a Bruker Avance III 500 MHz with TMS as an internal standard (unless noted otherwise). The products were purified by flash column chromatography using Teledyne Ultra Pure Silica Gel (230–400 mesh) on a Teledyne Isco CombiFlash Rf using hexanes/EtOAc or DCM/methanol as eluents. Spectroscopy-grade solvents were used. Solutions were degassed by purging with nitrogen. The irradiations were carried out in an in-house-built merry-go-round photoreactor, equipped with 365 nm Nichia UV LEDs.

Absorption spectra were measured with Cary 100Bio UV-visible spectrophotometer and Beckman DU640 spectrophotometer. Fluorescence was measured with Varian Cary Eclipse fluorescence spectrophotometer. Fluorescence quantum yields (QYs) were determined by comparing the integrated intensities of the fluorescence spectra ( $\lambda_{\text{ex}} = 350$  nm) with that of standard quinine sulfate in 0.1 M aqueous sulfuric acid ( $\Phi_{\text{std}} = 0.577$ ,  $\lambda_{\text{ex}} = 350$  nm) over a range of concentrations.

The QYs of the reactions were determined by comparing the conversion rate of the 0.01 M solution of the photoprecursor and the benzophenone–benzhydrol actinometer system,<sup>25</sup> reduction of a 0.1 M solution of benzophenone in a 1 M solution of benzhydrol,  $\Phi_{\text{BP}} = 0.57$ .

Rates of quenching of the reaction rates with *trans*-piperylene<sup>26</sup> in benzene and molecular oxygen in acetonitrile were determined by measuring the conversion rates for a 0.01 M solution of photoprecursors in the presence of varied concentrations of the quencher.

The relative QYs of the reaction in different solvents were measured by comparing the conversion rates of the reactions of the same concentration in acetonitrile and benzene and also in the absence of hexamethylphosphoramide (HMPA) or with 1 vol % of HMPA. The concentration of photoprecursors, 10 mM, was chosen to ensure that more than 99% of incident light was absorbed.

Fluorescence decay profiles were recorded using a time-correlated single-photon counting (TCSPC) spectrometer (Horiba Jobin Yvon IBH). PicoBrite (375 nm, 1 MHz repetition rate, and 50 ps pulse width) was used as an excitation source, and an MCP photomultiplier (Hamamatsu R3809U-50) was used as the detector. The details of the experimental setup and methods of analysis of the decay curves using a nonlinear least-squares iteration procedure were described previously.<sup>27,28</sup> Transient absorption measurements were attempted with a laser flash photolysis (LFP) setup equipped with a Q-switched Nd:YAG laser (pulse width of ~8 ns) from Spectra-Physics, Quanta-Ray INDI series, and the LKS.60 Applied Photophysics spectrometer. The spectrometer consisted of a 150 W pulsed xenon lamp, programmable f/3.4 grating monochromator (Agilent), 600 MHz digitized oscilloscope, and R-928 photomultiplier tube. The solution was excited by the third harmonic (355 nm) of the laser, and the optical densities of the sample solutions were maintained at about 0.3 at the excitation wavelength in a quartz cuvette of

path length 1 cm. The experiments were carried out in degassed acetonitrile.

**Computational Methods.** The Gaussian 09, rev. A02, computational package was used for all DFT, CISD, and CASSCF computations.<sup>29</sup> The initial geometries were generated with Chem3D and preoptimized with the Sybyl force field. Full geometry optimizations were carried out with a DFT B3LYP/6-311+G(d,p) method, with the exception of the OH–N proton transfer in the ground state, where the O–H distance scan was carried out with CISD/6-311+G(d,p) geometry optimization. Time-dependent (TD) DFT calculations for vertical singlet excited states were performed at the TD B3LYP/6-311+G(d,p) level of theory, using either ground-state or triplet-state geometries.

The spin-orbit coupling (SOC) calculations were carried out with 0.5–0.5 triplet–singlet state averaging using Robb's CASSCF approach as implemented in Gaussian 09. Both active spaces of (6,6) and (8,10) were used.

## 3. RESULTS

**3.1. QY Study.** Absolute QYs were determined by comparison of the conversion rate of thoroughly degassed 0.01 M solution of photoprecursors **1a–1f**, **2a,b**, **3a,b**, **4a**, **5a**, **6–8** with the benzophenone–benzhydrol actinometer.<sup>25</sup> The typical plots of conversion versus time are shown in Figure 3.

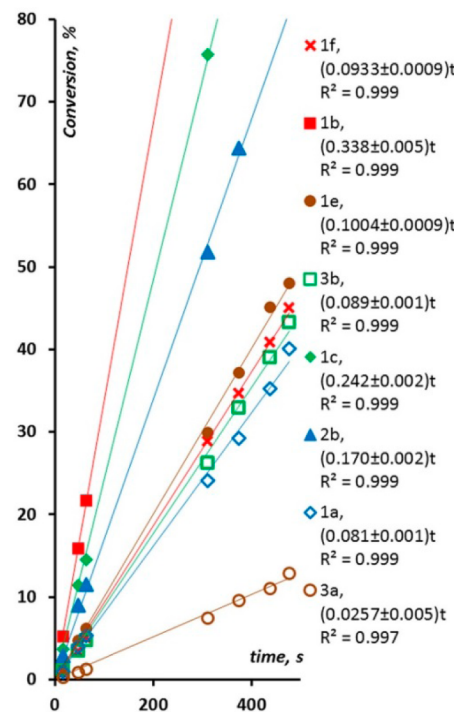
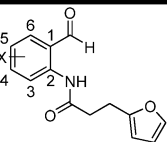
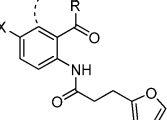
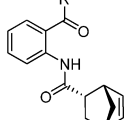


Figure 3. A typical carousel run for cyclization of photoprecursors **1a–c,e,f**, **2b**, **3a,b**.

The conversion was measured by calculating the ratio of integrated proton peaks in <sup>1</sup>H NMR peaks corresponding to photoproducts versus the sum of the integral values of photoprecursor and photoproducts. The absolute QYs, Table 1, were obtained from the slope ratios normalized to the known QY of the actinometer.

The highest QY,  $\Phi_r = 0.75$ , was obtained for the derivative of aminobenzaldehyde, **1b**, bearing a bromo substituent in the aromatic ring. The change in the position of Br from 5 to 4

Table 1. Absolute QYs of Photocyclization

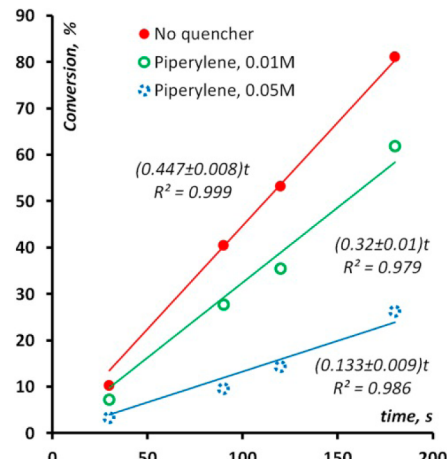
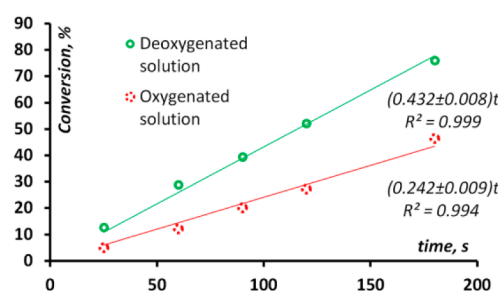
	QY
<b>1b</b> , X=5-Br	0.75±0.06
<b>1c</b> , X=5-I	0.54±0.02
<b>1d</b> , X=5-Cl	0.32±0.01
<b>1e</b> , X=4-Br	0.22±0.02
<b>1f</b> , X=5-(pyridin-3-yl)	0.21±0.02
<b>1a</b> , X=H	0.18±0.01
<hr/>	
	
<b>2b</b> , X=Br, R = -CH <sub>2</sub> CH <sub>2</sub> CH <sub>2</sub> -	0.38±0.04
<b>3b</b> , X=Br, R=CH <sub>3</sub>	0.20±0.02
<b>2a</b> , X=H, R = -CH <sub>2</sub> CH <sub>2</sub> CH <sub>2</sub> - (tetralone-derived)	0.18±0.01
<b>3a</b> , X=H, R=CH <sub>3</sub>	0.058±0.004
<b>4a</b> , X=H, R = -CH <sub>2</sub> CH <sub>2</sub> - (indanone-derived)	0.043±0.002
<b>5a</b> , (anthraquinone derived)	<0.01
<hr/>	
	
<b>6</b> , R=H	0.080±0.004
<b>7</b> , R=CH <sub>3</sub>	0.027±0.001
<b>8</b> , R=Ph	<0.01

resulted in a considerable decrease of QY to 0.22. Instructively, the iodine-substituted compound **1c** demonstrates a lower QY, 0.54, than its Br-substituted counterpart **1b**.

The reaction rate is also sensitive to the nature of the carbonyl moiety, with aldehyde-derived substrates **1** exhibiting much higher QYs than the structurally rigid tetralone derivatives **2**. The acetophenone-based precursors **3** and **7** are less efficient. The derivatives of bis-aromatic ketones, benzophenone **8** and anthraquinone **5**, are the least reactive in the series.

The nature of the unsaturated azaxylenophile pendant also plays a role; 3-(2-furyl)propanamides are generally more reactive than the norbornenyl-acetyl amide pendants in **6–8**.

**3.2. Quantum Efficiency in the Presence of Triplet Quenchers.** Photoinduced cyclization of photoprecursor **1b** in the presence of known triplet quenchers *trans*-piperlylene<sup>26</sup> and molecular oxygen was carried out. In both cases, a significant deceleration of product formation was observed, Figures 4 and 5.

Figure 4. *trans*-Piperylene quenching of **1b** in benzene.Figure 5. O<sub>2</sub> quenching of **1b** in acetonitrile.

Irradiation of a 0.01 M solution of **1b** with and without a quencher in a carousel UV LED reactor was monitored by NMR. Under these conditions, the ratio of the slopes in Figures 4 and 5 corresponds to the relative QYs with or without the quencher. The 8 mM concentration of O<sub>2</sub><sup>30</sup> in acetonitrile was achieved by saturating the sample via oxygen gas bubbling.

Stern–Volmer analysis of the data yielded the value of K<sub>SV</sub> of 99 ± 5 M<sup>-1</sup> s<sup>-1</sup> for quenching with O<sub>2</sub> in acetonitrile and 57 ± 8 M<sup>-1</sup> s<sup>-1</sup> for quenching with *trans*-piperlylene in benzene. If one assumes a diffusion-controlled limit for the quenching process (*k*<sub>dif</sub> = 1.1 × 10<sup>10</sup> M<sup>-1</sup> s<sup>-1</sup> in benzene at 25 °C and 1.9 × 10<sup>10</sup> M<sup>-1</sup> s<sup>-1</sup> in acetonitrile),<sup>31</sup> the lifetime of the species being quenched is 5.2 ± 0.3 ns in acetonitrile and 5.7 ± 0.8 ns in benzene.

**3.3. Effect of Hydrogen Bonding.** In order to evaluate the effect of hydrogen-bonding interactions, 0.01 M solutions of photoprecursor **9** in acetonitrile and benzene were prepared with and without HMPA (1 vol %). The samples were degassed and irradiated in a carousel UV LED photoreactor. The conversion was followed by <sup>1</sup>H NMR and plotted against time, as shown in Figure 6. The slope ratios show nearly 2-fold (1.93) acceleration in a polar hydrogen-bonding solvent, acetonitrile, as compared with nonpolar benzene and 5.6 times acceleration in the presence of 1 vol % of HMPA. The fastest reaction, 10.5 times faster than the reference (benzene without addition of HMPA), was observed in acetonitrile with 1 vol % of HMPA. The effect of hydrogen-bonding solvents on extending the lifetimes of triplet hydroxy-xylylenes generated via ESIPT is precedented in the literature.<sup>20</sup>

**3.4. Steady-State Spectroscopy.** UV-vis spectra of *o*-formyl- and *o*-acylbenzamides are characterized by a strong absorption band with a maximum at 336–350 nm. Judging

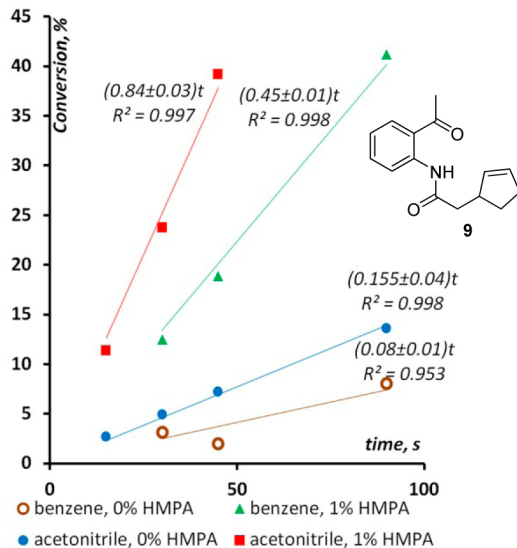


**Figure 6.** Effect of solvent polarity and addition of HMPA on the reaction of 9.

from the relatively large molar absorption coefficient,  $4900\text{ M}^{-1}\text{ cm}^{-1}$  for compound **2b**, we assign this band to a ( $\pi,\pi^*$ ) absorption.<sup>32</sup> The solvent dependence of the absorption spectra is in full agreement with the data previously published for 1-(acylamino)anthraquinones<sup>33</sup> and acetophenones.<sup>34</sup> With increased solvent polarity (dichloromethane to acetonitrile), a hypsochromic shift is observed, which may be indicative of intermolecular hydrogen bonding with solvent.

Fluorescence spectra of aldehydes **1a**, **6**, **10**, and **11ab** (see Figure 7) exhibit very weak, almost nondiscernable, ESIPT

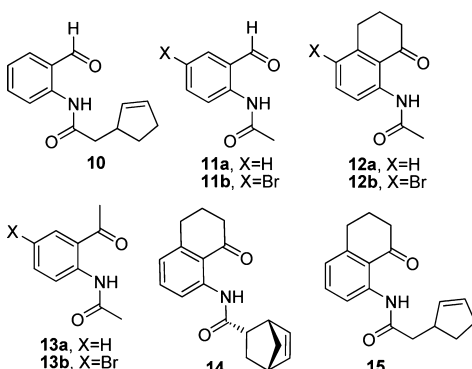


**Figure 7.** Compounds 10–15.

bands. The short-wavelength emission maxima are found at 392–417 nm depending on substitution on the amide, Figure 8. At the same time tetralone- and acetophenone-derived photoprecursors **2a,b**, **3a,b**, and **12–15** are characterized by dual fluorescence, the normal and the Stokes-shifted ESIPT fluorescence bands, with maxima centered at around 388–433 nm and 525–541 nm, respectively. The Stokes shift values ranged from 9600 to 11300  $\text{cm}^{-1}$ .

The tetralone derivatives, which do not have a rotatable carbonyl, exhibit small variations of the intensity of the ESIPT band depending on the amide pendant. However, unlike the case with the aldehydes, the ESIPT band in all tetralones is always prominent. What's most important, the ratios of the two bands are equal for furanpropanamidotetralone **2a**, which is

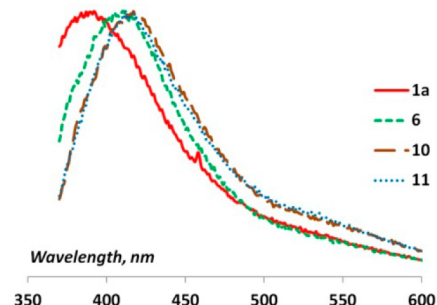


**Figure 8.** Normalized fluorescence spectra of aldehydes **1a**, **6**, **10**, and **11** in dichloromethane.

capable of intramolecular cycloaddition, and the acetamidotetralone **12a**, which is photoinactive (see Figure 9).

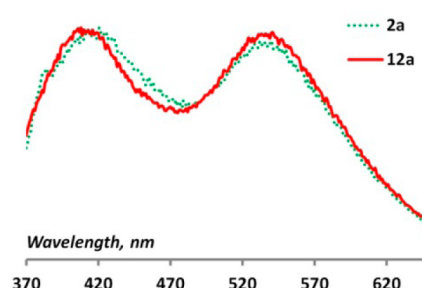


**Figure 9.** Normalized fluorescence spectra of furanpropanamidotetralone **2a** (photoreactive) and acetamidotetralone **12a** (photoinactive).

However, bromo substitution in the *para* position to the amido group of the aromatic ring causes a profound effect on the ratio of intensities of the two bands, Figure 10.

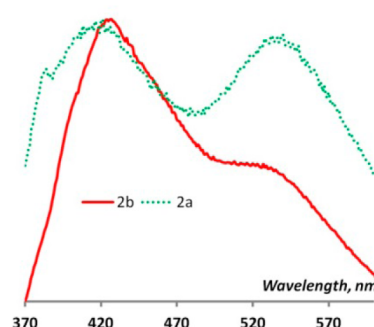


**Figure 10.** Normalized fluorescence spectra of tetralone **2a** and bromotetralone **2b**.

Unsubstituted tetralone derivative **2a** has a 1.1:1 ratio of the short- to long-wavelength emission intensities, while bromo-substituted **2b** exhibits the ratio of 1.8:1. Both are equipped with the same furanpropanoyl pendant.

We have measured the absolute QY of fluorescence for compound **2b**,  $\Phi_{\text{FL}} = 0.0033$ , using the standard quinine sulfate, for which the fluorescence QY is known (0.577). This is in line with values of 0.0011–0.034 reported by Barbara.<sup>8</sup>

**3.5. Time-Correlated Single Photon Counting.** The fluorescence decay profiles were measured by the picosecond single-photon counting method. The 0.001 M solutions of photoprecursors **1a**, **1b**, and **2b** were prepared in acetonitrile and degassed. Decay profiles are shown in Figure 11.

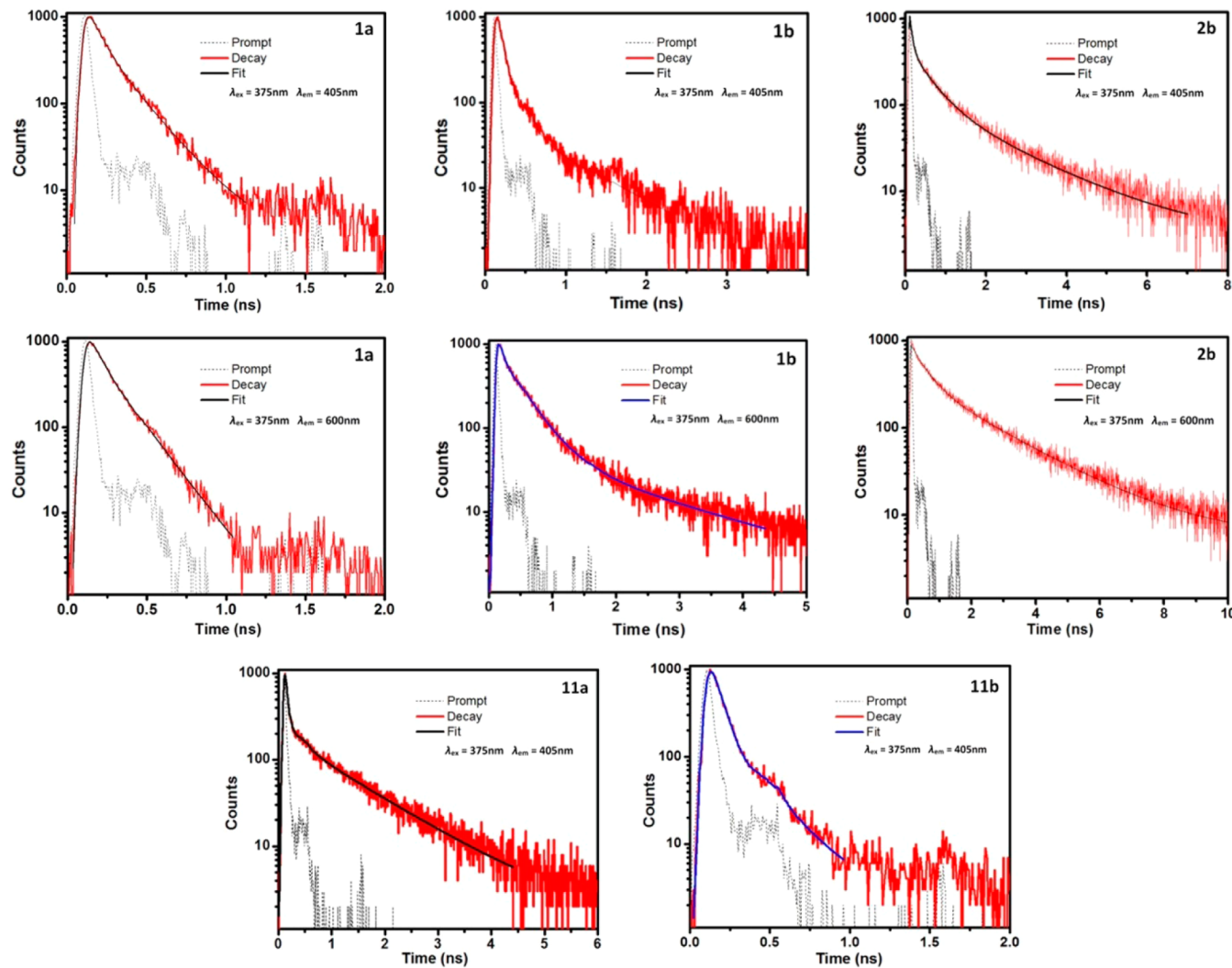


**Figure 11.** Picosecond TCSPC decay profiles of degassed acetonitrile solutions of **1a**, **1b**, **2b**, **11a**, and **11b** and multiexponential fits to the data.

**Table 2. Fluorescence Time Constants of the Samples Estimated from the Decay Profiles Collected at 405 and 600 nm**

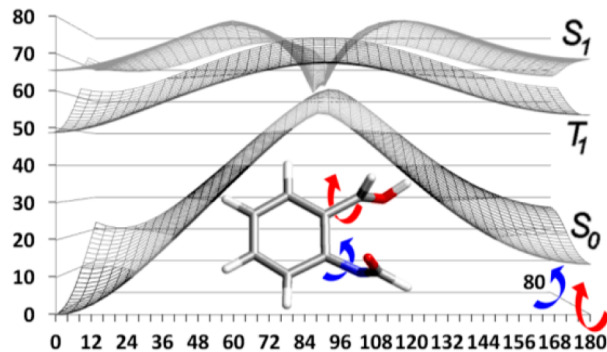
	405 nm				600 nm			
	$\tau_1$	$\tau_2$	$\tau_3$	$\chi^2$	$\tau_1$	$\tau_2$	$\tau_3$	$\chi^2$
<b>1b</b>	50	200	960	1.19	74	300	1500	1.16
<b>2b</b>	65	482	1800	1.09		459	1840	1.14
<b>1a</b>	72	204		1.22	61	182		1.03
<b>11a</b>	<50(23)	234	1160	1.09				
<b>11b</b>	<50(47)	234		1.13				

The decay data are summarized in Table 2. The fluorescence decay profiles were fitted with two- or three-exponential decay terms.

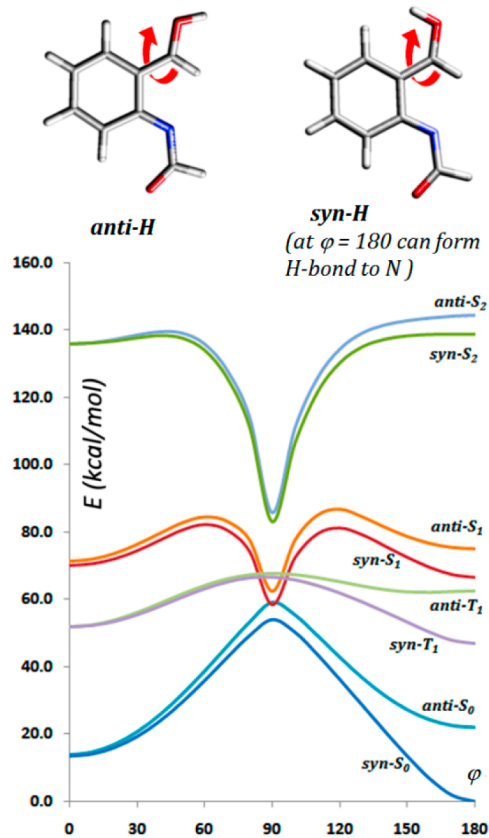
**3.6. DFT and Ab Initio Calculations.** The model system, azaxylylene derived from *N*-formylaminobenzaldehyde, with the *anti* orientation of the benzylic OH group to prevent back proton transfer was fully optimized in the ground state at the B3LYP/6-311+G(d,p) level of DFT theory. The optimized structure with all internal coordinates frozen was used for a 2D rigid torsional scan to visualize the approximate relative energies of the three lowest PESs, the ground state  $S_0$ , the first excited state  $S_1$  (TD DFT), and the lowest triplet  $T_1$ , Figure 12.

Figure 13 shows a more nuanced picture where hydroxymethylene rotation is followed in two species, *syn*-H, that is, the dihedral  $\angle H-O-C-C$  is  $0^\circ$  (this OH rotamer can form a hydrogen bond with nitrogen) and *anti*-H (not capable of hydrogen bonding). Even in the diradicaloid triplet species, the stabilizing effect of the hydrogen bonding is more than 10 kcal/mol, presumably because the flat conformation of the triplet is ( $\pi,\pi^*$ ), and the lone pair on the nitrogen atom is intact. A similar trend is observed for the  $S_1$  state, where the energy difference between the hydrogen-bonded *syn*-H/*syn*-OH conformer and the *anti*-H/*syn*-OH conformer is approximately 5–7 kcal/mol.

We also modeled back proton transfer in the *syn*-H/*syn*-OH conformer by stretching the OH bond from its optimized value



**Figure 12.** 2D torsional scan in the parent azaxylylene. The front horizontal axis is annotated with the red arrow—hydroxybenzyl rotation from 0 to 180°. Rotation of the amide fragment (the second horizontal axis) is annotated with the blue arrow, 80–180°.



**Figure 13.** Hydroxymethylene rotation in *syn*- (capable of the intramolecular hydrogen bonding) and *anti*-H species (not capable of hydrogen bonding); B3LYP/6-311+G(d,p) and TD B3LYP/6-311+G(d,p).

of 0.9 Å. As Figure 14 shows, the *syn*-H/*syn*-OH azaxylylene is a shallow minimum on the  $S_1$  PES (TD DFT). However, we did not find a minimum on the ground-state surface at the B3LYP/6-311+G(d,p) level of DFT theory nor even with CISD/6-311+G(d,p). The calculations show only a slight change in the curvature of the  $S_0$  PES along this reaction coordinate. The back proton transfer seems to occur without any energy barrier in the ground state.

The difference in QYs of 5- (**1b**) versus 4-bromo (**1e**) substituted substrates prompted a closer computational look into their parent truncated species (i.e., the formamides). We fully optimized the geometry of their respective *syn*-H/*anti*-OH

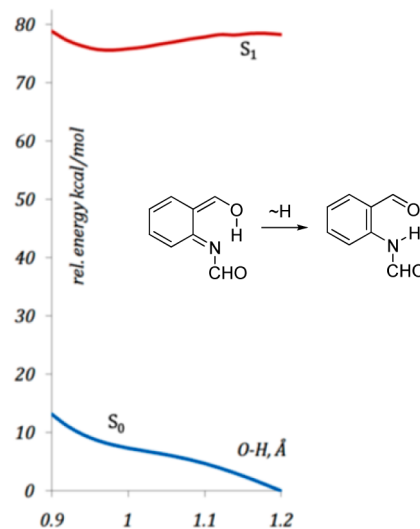


**Figure 14.** Stretching the OH bond in the *syn* conformer. The ground-state energies are CISD/6-311+G(d,p). The  $S_1$  PES is TD B3LYP/6-311+G(d,p).

and *anti*-H/*anti*-OH conformers in the triplet state and ran a relaxed scan on the triplet PES rotating the hydroxymethylene. The overall shape of the PES was very similar to what was found earlier for the parent unsubstituted azaxylylene shown in Figure 12. The Mulliken spin density on bromine atoms was however very different for the two isomers; as Figure 15 shows,

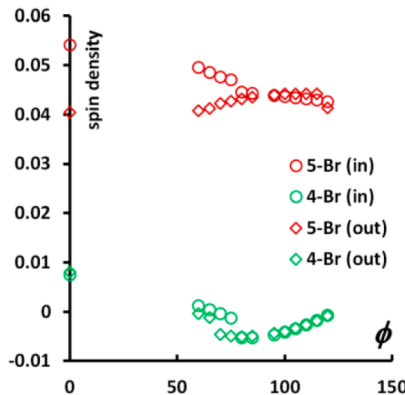


**Figure 15.** Mulliken spin densities on Br atoms in 4- and 5-substituted azaxylylenes as a function of rotation of hydroxymethylene; torsional angle  $\phi$ , HOCH-C<sub>aryl</sub>; B3LYP/6-311+G(d,p).

spin density on Br in the 5-substituted isomer is almost an order of magnitude higher than that in the 4-bromo compound. This is true both for the conformations with hydroxymethylene rotated out of the plane of the molecule and for  $\phi = 0^\circ$ .

SOC values, computed with CASSCF(6,6) and CASSCF-(10,8), 0.5–0.5 state average, for 85 and 95° rotation of hydroxymethylene were also in keeping with the spin density trend on Br atoms, Table 3. The SOC values for the 4-bromo-substituted species were 1.3–3 times smaller than that of 5-bromoazaxylylene, which potentially can account for up to a 9-fold decrease in the rate of ISC, that is,  $1.7 < |\text{SOC}^{5\text{Br}}|^2 / |\text{SOC}^{4\text{Br}}|^2 < 9$ .

**Table 3.** Spin-orbit coupling ( $\text{cm}^{-1}$ ) in 5-Br- vs 4-Br- isomers of N-formyl azaxylylene at different rotation of hydroxymethylene

active space →	$\phi = 95^\circ$		$\phi = 85^\circ$	
	6,6	10,8	6,6	10,8
5-Br-in	1.1	1.2	0.5	0.6
4-Br-in	0.5	0.5	0.2	0.2
5-Br-out	0.9	1.0	0.4	0.5
4-Br-out	0.6	0.6	0.3	0.3

#### 4. DISCUSSION

There were several early indications that the mechanism of intramolecular cycloadditions of hydroxyazaxylyenes, photo-generated via ESIPT, may be stepwise. In our early work, we observed that for slow-reacting aminoacetophenone derivatives, outfitted with a cyclopentenylacetyl unsaturated pendant, up to 25% of the product at ambient temperature is derived from a radical disproportionation channel,<sup>21</sup> Figure 16a, indicating the

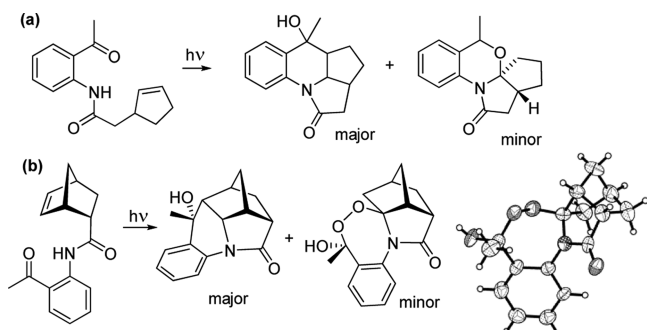


**Figure 16.** Photoinduced cyclization in furanpropanamide of amino-benzaldehyde. The X-ray structure of the minor endoperoxide is shown.

nitrogen-centered radical attack on the double bond as the initial step. Additionally, in a similar reaction with a norbornene pendant, the 1,6-diradical derived from such an initial attack can rearrange and be trapped with oxygen (Figure 16b shows the ORTEP drawing of the trapped endoperoxide). Figure 17 shows a plausible mechanistic rationale for the formation of the minor aminal as a result of intramolecular radical disproportionation with subsequent addition of benzylic alcohol to the formed N-acyl enamine. It appears that the excited state of the

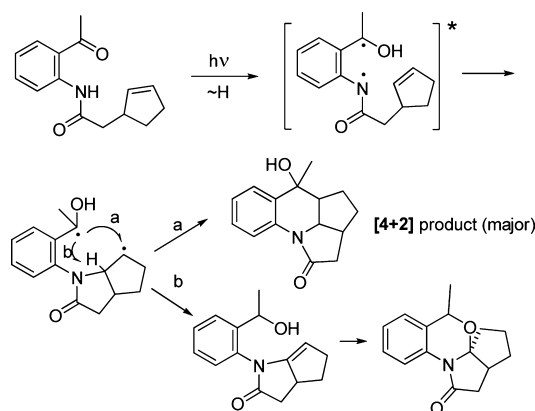


**Figure 17.** Photoinduced cyclization in furanpropanamide of amino-benzaldehyde.

azaxylylene is better represented as a diradicaloid species, with unshared electronic density located on the nitrogen and benzylic carbon.

There are several reasons to rule out the ground-state reaction of azaxylylenes. The products of [4 + 4] cycloaddition indicate either a nonconcerted or an excited-state process. One may entertain the idea that the [4 + 4] and [4 + 2] reactions with furan-bearing pendants are two distinct excited-state and ground-state processes. This scenario is unlikely for several reasons. As our computational results demonstrate, there is no barrier to the back proton transfer on the ground-state PES, making the ground-state reaction questionable. Also, the ESIPT-generated hydroxyazaxylyenes do not form cycloadducts with electron-deficient alkenes. In contrast, their all-carbon counterparts, xylylenes, as dienols react with maleic anhydride or maleimides even in a bimolecular fashion. Up to date, we were unable to engage hydroxyazaxylyenes in an intermolecular reaction. Azaxylylenes lacking the terminal hydroxy group were generated by others via alternative pathways and were shown to undergo bimolecular [4 + 2] cycloadditions with enol ethers in the ground state<sup>35</sup> via inverse electron-demand aza-Diels–Alder reactions. It appears that in the case of ESIPT-generated azaxylylenes, the hydroxy group on the terminal carbon of the azadiene moiety significantly decreases the ground-state reactivity to a point that the cycloaddition reactions cannot compete with fast back proton transfer that is available for these species. At the same time, hydroxyazaxylylenes are not as nucleophilic as hydroxy-xylylenes; therefore, they do not react with electron-deficient alkenes in the ground state either.

As the Results section shows, in order to test our excited-state mechanistic hypotheses and refine our understanding of underlying processes, we carried out the steady-state and time-resolved spectroscopic study, the fluorescence QY and the cycloaddition reaction quantum studies, and the computational DFT and ab initio study.

According to Barbara, ESIPT in aromatic *o*-amidoketones occurs within 300 fs; therefore, both emission bands are established within under 1 ps and serve as reporters for subsequent processes.<sup>8</sup> Unlike the convenient anthraquinone derivatives studied in the past, aminoketones and aldehydes are not ideal for time-resolved studies as the ESIPT bands in their emission spectra are very weak. This problem is aggravated by the low fluorescence QYs. However, we attempted TCSPC experiments that showed multiexponential decay complicated by the overlap of the two emission bands. Measuring decays separately at 405 and 600 nm helped to assign the processes.

The shorter-wavelength emission showed a major very fast component of  $\tau \approx 50\text{--}70$  ps accounting for 60–90% of emitting species. This could plausibly be assigned to fast internal conversion of the initially excited species in conformations not conducive to proton transfer. Measurements at 600 nm show a larger component decaying at  $\tau \approx 200\text{--}480$  ps and longer 1–2 ns lifetimes. The 200–480 ps decays were “bleeding” into the short-wavelength measurements but accounted for smaller percentages of emitting species there. These decays could correspond to the internal conversion in the tautomeric form (Tobita<sup>36</sup> has assigned 409 ps in trifluoroacetylalamido-acetophenone to internal conversion in the enol form) or ISC.

While it is difficult to confidently assign these lifetimes, it is evident that the introduction of the furanpropanamido pendant does not have significant impact on the rates as compared with

the acetamido controls. The main conclusion derived from the time-resolved study is that it is highly unlikely that there is a considerable singlet-state reaction channel for the cycloaddition reactions.

As follows from Table 1 aminobenzaldehyde derivatives showed the highest QYs of product formation, with 5-bromobenzaldehyde topping the list ( $\Phi_r = 0.75$ ). One evident trend here is that any substitution at carbonyl in the photoprecursor (i.e., the benzylic position in azaxylenes) has a detrimental impact on cycloaddition. Less stabilized and less sterically hindered hydroxybenzylic radical is clearly more reactive, readily completing the cycloaddition process.

A finer detail is that the aminotetralone-derived photoprecursor **2a** reacted more efficiently ( $\Phi_r = 0.15$ ) than amidoacetophenone **3a** ( $\Phi_r = 0.06$ ). Carbonyl rotation is not available to the tetralone derivative, which has rotational freedom only for the amido moiety. Rotation of the deprotonated amide may slow down the back proton transfer, but it is unlikely that a cycloaddition reaction can compete with it on the singlet PES. However, if there is ISC to the triplet, facilitated by the amide rotation, it can explain the slow back proton transfer and competitive nitrogen attack on the tethered unsaturated moiety. Ichinose and Nakayama<sup>37</sup> studied “ESIPT-type” phosphorescence in 2-aminobenzophenone and concluded, based on the observation that both phosphorescence bands decayed independently, that ESIPT via triplet state is “not important.” In the context of this study, this is a critical observation.

Bromo substitution was found to consistently improve the QYs of photoinduced cycloadditions. Additionally, from the steady-state fluorescence of tetralone derivatives, Figure 10, it is evident that the introduction of bromine in the aromatic ring significantly quenches the ESIPT emission band. Given the consensus in the literature that both bands are established within subpicosecond times<sup>8,9</sup> and that the triplet-state proton transfer is negligible, a plausible explanation for the ratiometric changes in the emission profiles shown in Figure 10 is that the bromo substitution induces fast ISC in the tautomer due to elevated SOC. Regrettably, we could not obtain TCSPC data for the unbrominated parent, amidotetralone. However, bromination more than doubles the QY of the cycloadducts formation from 0.15 to 0.38 in the tetralone series.

This effect is partially related to Br’s electronegativity, making the N-centered radical more electrophilic and more reactive toward the furanyl pendant. Comparison of the QYs for 5-chloro- ( $0.32$ , **1d**), 5-bromo- ( $0.75$ , **1b**), and 5-iodo- ( $0.54$ , **1c**) furanpropanamido benzaldehydes helps explain the fine interplay of the two effects, the heavy atom effect on SOC and the electron-withdrawing effect enhancing the reactivity of the N-centered radical toward the electron-rich dienic system of furan. Table 4 summarizes Pauling’s electronegativities and atomic SOC values for the three halogens.

We hypothesize that the optimal combination of elevated SOC and high electronegativity results in the highest QY of

photoinduced cyclization for the bromo-substituted photoprecursor **1b**. The iodo precursor suffers from lower electronegativity, while the chloro compound has an order of magnitude smaller atomic SOC than the iodo precursor.

Triplet photocycloadditions are of course preceded.<sup>38</sup> Another evidence pointing to triplet cycloaddition is the oxygen (in acetonitrile) and piperylene (benzene) quenching experiments. Both quenchers impede the formation of cycloadducts from **1b** considerably. Assuming diffusion-controlled quenching rates, one derives triplet lifetimes of  $\tau \approx 5.2\text{--}5.7$  ns from the Stern–Volmer  $K_{SV}$  values found in the Results section. This is a realistic lifetime for a triplet decaying via a fast *intramolecular* attack of the N-centered radical on the tethered unsaturated pendant.

Finally, Table 1 shows more than a 3-fold difference in QYs of product formation between 4-bromo- ( $\Phi_r = 0.22$ , **1e**) and 5-bromo-substituted ( $\Phi_r = 0.75$ , **1b**) photoprecursors. Our theoretical study shows that in the triplet state, the Mulliken spin density on Br atoms in the 5-bromo isomer is 1 order of magnitude greater than that of 4-bromo isomer for a variety of rotated out and flat conformations. This can provide an indirect rationale for higher rates of ISC via the heavy atom effect, which can only be realized if there is high spin density on the heavy atom in the receiving state. This is necessary but not sufficient evidence. We also calculated the actual SOC elements for the geometries where the hydroxymethylene group is rotated out of plane of the molecule, that is, in the vicinity of the likely surface-hopping geometry. For two torsional angles of  $85^\circ$  and  $95^\circ$ , the total magnitudes of SOC matrix elements were 1.3–3 times higher for the 5-bromo-substituted species than those for the 4-bromo-substituted. Because it is the square of the matrix element that goes into the numerator for the rates of nonadiabatic transitions, other conditions being equal, these differences are sufficient to explain up to 9-fold rate differences (a 3-fold QY difference is observed).

## 5. CONCLUSIONS

Amides of aromatic *o*-ketones and aldehydes undergo fast and efficient ESIPT into their tautomeric form, azaxylylene, followed by ISC into the triplet manifold. With the attached furanpropanoyl, the triplet azaxylylene has a lifetime of up to 5 ns as it is quenched via a fast intramolecular reaction with the unsaturated furyl pendant resulting in subsequent cycloaddition or further disproportionation or intermolecular radical trapping. There are no indications that the cycloaddition reaction occurs in the singlet excited state. It is also highly unlikely that the cycloadditions of C-hydroxy-substituted azaxylenes can occur in the singlet ground state.

As the initial attack of the N-centered radical is important for a high yielding reaction, substituents that increase the yields of triplets and at the same time increase the electronegativity of the radical improve QYs of this photoinduced cycloaddition. The reaction is completed via another ISC and the intramolecular collapse of the singlet radical pair to form the products of formal [4 + 2] or [4 + 4] cycloadditions. A less substituted hydroxybenzylic radical favors radical recombination as opposed to disproportionation or intermolecular trapping, thus improving the yields of the desired heterocyclic products. This is one of the reasons why the photoprecursors derived from *o*-amidoaldehydes undergo efficient cycloaddition reactions.

**Table 4. QYs of Photocycloadditions in **1b–d** and Atomic SOC Values and Pauling’s Electronegativity for Cl, Br, and I**

	Cl	Br	I
electronegativity	3.16	2.96	2.66
atomic SOC, <sup>31</sup> cm <sup>-1</sup>	587	2460	5069
QY, cycloaddition	0.32 ( <b>1d</b> )	0.75 ( <b>1b</b> )	0.54 ( <b>1c</b> )

## ■ ASSOCIATED CONTENT

### § Supporting Information

Additional experimental and computational data, including synthesis details, photophysical data, and NMR spectra. This material is available free of charge via the Internet at <http://pubs.acs.org>.

## ■ AUTHOR INFORMATION

### Corresponding Author

\*E-mail: akutatel@du.edu. Tel: +1-303-871-2995.

### Author Contributions

<sup>†</sup>O.A.M. and W.C.C. contributed equally.

### Notes

The authors declare no competing financial interest.

## ■ ACKNOWLEDGMENTS

Support of this research by the National Science Foundation, CHE-1362959, and DST (Government of India) is gratefully acknowledged.

## ■ REFERENCES

- (1) Ritter, J.; Borst, H.-U.; Linder, T.; Hauser, M.; Brosig, S.; Bredereck, K.; Stiener, U. E.; Kuhn, D.; Kelemen, J.; Kramer, H. E. A. Substituent Effects on Triplet Yields in Aminoanthraquinones: Radiationless Deactivation via Intermolecular and Intramolecular Hydrogen Bonding. *J. Photochem. Photobiol. A* **1988**, *41*, 227–244.
- (2) Inoue, H.; Hida, M.; Nakashima, N.; Yoshihara, K. Picosecond Fluorescence Lifetimes of Anthraquinone Derivatives. Radiationless Deactivation via Intra- and Intermolecular Hydrogen Bonds. *J. Phys. Chem.* **1982**, *86*, 3184–3188.
- (3) Flom, S. R.; Barbara, P. F. Proton Transfer and Hydrogen Bonding in the Internal Conversion of  $S_1$  Anthraquinones. *J. Phys. Chem.* **1985**, *89*, 4489–4494.
- (4) Land, E. J.; McAlpine, E.; Sinclair, R. S.; Truscott, T. G. Triplet Excited States of 1,4-Dissubstituted Anthraquinones: Possible Evidence for Association of Quinones in Solution. *J. Chem. Soc., Faraday Trans. 1* **1976**, *172*, 2091–2100.
- (5) Hulme, B. E.; Land, E. J.; Phillips, G. O. Pulse Radiolysis of 9,10-Anthraquinones. Part 2. — Triplet Excited States. *J. Chem. Soc., Faraday Trans. 1* **1972**, *68*, 2003–2012.
- (6) Dearman, H. H.; Chan, A. Photochemistry of Substituted Anthraquinones. *J. Chem. Phys.* **1966**, *44*, 416–417.
- (7) Srivatsavoy, V. J. P.; Venkataraman, B. Laser Flash Photolysis of 1-Acetylaminanthraquinone. *Chem. Phys. Lett.* **1990**, *174*, 406–410.
- (8) Smith, T. P.; Zaklika, K. A.; Thakur, K.; Walker, G. C.; Tominaga, K.; Barbara, P. F. Spectroscopic Studies of Excited-State Intramolecular Proton Transfer in 1-(Acylamino)anthraquinones. *J. Phys. Chem.* **1991**, *95*, 10465–10475.
- (9) Schmidtke, S. J.; Underwood, D. F.; Blank, D. A. Probing Excited-State Dynamics and Intramolecular Proton Transfer in 1-Acylaminoanthraquinones via the Intermolecular Solvent Response. *J. Phys. Chem. A* **2005**, *109*, 7033–7045.
- (10) Nicolaou, K. C.; Gray, D. L. F.; Tae, J. Total Synthesis of Hamigerans and Analogues Thereof. Photochemical Generation and Diels–Alder Trapping of Hydroxyl-*o*-quinodimethanes. *J. Am. Chem. Soc.* **2004**, *126*, 613–627.
- (11) Nicolaou, K. C.; Gray, D. L. F. Total Synthesis of Hybocarpone and Analogues Thereof. A Facile Dimerization of Naphthazarins to Pentacyclic Systems. *J. Am. Chem. Soc.* **2004**, *126*, 607–612.
- (12) Nicolaou, K. C.; Gray, D. L. F. Total Synthesis of Hybocarpone. *Angew. Chem., Int. Ed.* **2001**, *40*, 761–763.
- (13) Nicolaou, K. C.; Gray, D. L. F.; Tae, J. Total Synthesis of Hamigerans: Part 1. Development of Synthetic Technology for the Construction of Benzannulated Polycyclic Systems by the Intermolecular Trapping of Photogenerated Hydroxyl-*o*-quinodimethanes and Synthesis of Key Building Blocks. *Angew. Chem., Int. Ed.* **2001**, *40*, 3675–3678.
- (14) Kraus, G. A.; Wu, Y. Hydrogen Atom Abstraction in Organic Synthesis. A Formal Total Synthesis of Racemic Podophyllotoxin. *J. Org. Chem.* **1992**, *57*, 2922–2925.
- (15) Quinkert, G.; Stark, H. Stereoselective Synthesis of Enantiomerically Pure Natural Products — Estrone as Example. *Angew. Chem., Int. Ed.* **1983**, *22*, 637–655.
- (16) Prabhakar, S.; Lobo, A. M.; Tavares, M. R.; Oliveira, I. M. C. Total Synthesis of the Alkaloids ( $\pm$ )-Alpigenine and ( $\pm$ )-*cis*-Alpigenine. *J. Chem. Soc., Perkin Trans. 1* **1981**, 1273–1277.
- (17) Quinkert, G.; Weber, W.-D.; Schwartz, U.; Dürner, G. A Photochemical Route to (7 $\pm$ )-Estrone. *Angew. Chem., Int. Ed.* **1980**, *19*, 1027–1029.
- (18) Quinkert, G.; Schwartz, U.; Stark, H.; Weber, W.-D.; Baier, H.; Adam, F.; Dürner, G. Asymmetric Total Synthesis of (+)-Estrone. *Angew. Chem., Int. Ed.* **1980**, *19*, 1029–1030.
- (19) Segura, J. L.; Martin, N. *o*-Quinodimethanes: Efficient Intermediates in Organic Synthesis. *Chem. Rev.* **1999**, *99*, 3199–3246.
- (20) Haag, R.; Wirz, J.; Wagner, P. J. The Photoenolization of 2-Methylacetophenone and Related Compounds. *Helv. Chim. Acta* **1977**, *60*, 2595–2607.
- (21) Mukhina, O. A.; Kumar, N. N. B.; Arisco, T. M.; Valiulin, R. A.; Metzel, G. A.; Kutateladze, A. G. Rapid Photoassisted Access to N,O,S-Polyheterocycles with Benzoazocine and Hydroquinoline Cores Intramolecular Cycloadditions of Photogenerated Azaxylylenes. *Angew. Chem., Int. Ed.* **2011**, *50*, 9423–9428.
- (22) Nandurkar, N. S.; Kumar, N. N. B.; Mukhina, O. A.; Kutateladze, A. G. Photoassisted Access to Enantiopure Conformationally Locked Ribofuranosylamines Spiro-Linked to Oxazolidino-Diketopiperazines. *ACS Comb. Sci.* **2013**, *15*, 73–76.
- (23) Kumar, N. N. B.; Mukhina, O. A.; Kutateladze, A. G. Photoassisted Synthesis of Enantiopure Alkaloid Mimics Possessing Unprecedented Polyheterocyclic Cores. *J. Am. Chem. Soc.* **2013**, *135*, 9608–9611.
- (24) Cronk, W. C.; Mukhina, O. A.; Kutateladze, A. G. Intramolecular Photoassisted Cycloadditions of Azaxylylenes and Photochemical Capstone Modifications via Suzuki Coupling Provide Access to Complex Polyheterocyclic Biaryls. *J. Org. Chem.* **2014**, *79*, 1235–1246.
- (25) Moore, W. M.; Hammond, G. S.; Foss, R. P. Mechanisms of Photoreactions in Solutions I. Reduction of Benzophenone by Benzydrol. *J. Am. Chem. Soc.* **1961**, *83*, 2789–2794.
- (26) Stephenson, L. M.; Hammond, G. S. Fate of the Excitation Energy in the Quenching of Fluorescence by Conjugated Dienes. *Pure Appl. Chem.* **1968**, *16*, 125–136.
- (27) Santhosh, K.; Samanta, A. Modulation of the Excited State Intramolecular Electron Transfer Reaction and Dual Fluorescence of Crystal Violet Lactone in Room Temperature Ionic Liquids. *J. Phys. Chem. B* **2010**, *114*, 9195–9200.
- (28) Banerjee, S.; Pabbathi, A.; Sekhar, M. C.; Samanta, A. Dual Fluorescence of Ellipticine: Excited State Proton Transfer from Solvent versus Solvent Mediated Intramolecular Proton Transfer. *J. Phys. Chem. A* **2011**, *115*, 9217–9225.
- (29) For the full Gaussian 09 citation, see the Supporting Information.
- (30) Maillard, B.; Ingold, K. U.; Scaiano, J. C. Rate Constants for the Reactions of Free Radicals with Oxygen in Solution. *J. Am. Chem. Soc.* **1983**, *105*, 5995–5999.
- (31) Murov, S. L.; Carmichael, I.; Hug, G. L. *Handbook on Photochemistry*; Marcel Dekker: New York, 1993; Section 16.
- (32) Yoshihara, T.; Shimada, H.; Shizuka, H.; Tobita, S. Internal Conversion of *o*-Aminoacetophenone in Solution. *Phys. Chem. Chem. Phys.* **2001**, *3*, 4972–4978.
- (33) Yatsuhashi, T.; Inoue, H. Molecular Mechanism of Radiationless Deactivation of Aminoanthraquinones through Intermolecular Hydrogen-Bonding Interaction with Alcohols and Hydroperoxides. *J. Phys. Chem. A* **1997**, *101*, 8166–8173.

- (34) Previtali, C. M.; Cosa, J. J.; Lema, R. H. Fluorescence of Ring-Substituted Phenyl Alkyl Ketones in Solution. *J. Lumin.* **1986**, *36*, 121–128.
- (35) Steinhagen, H.; Corey, E. J. Convenient and Versatile Route to Hydroquinolines by Inter- and Intramolecular aza-Diels–Alder Pathways. *Angew. Chem., Int. Ed.* **1999**, *38*, 1928–1931.
- (36) Shimada, H.; Nakamura, A.; Yoshihara, T.; Tobita, S. Intramolecular and Intermolecular Hydrogen-Bonding Effects on Photophysical Properties of 2'-Aminoacetophenone and Its Derivatives in Solution. *Photochem. Photobiol. Sci.* **2005**, *4*, 367–375.
- (37) Hagiri, M.; Ichinose, N.; Kinugasa, J.-I.; Iwasa, T.; Nakayama, T. Excited-State Intramolecular Proton Transfer (ESIPT)-Type Phosphorescence of 2-Aminobenzophenone in 77K Matrices. *Chem. Lett.* **2004**, *33*, 326–327.
- (38) Zeidan, T. A.; Kovalenko, S. V.; Manoharan, M.; Clark, R. J.; Ghiviriga, I.; Alabugin, I. V. Triplet Acetylenes as Synthetic Equivalents of 1,2-Bicarbenes: Phantom  $n,\pi^*$  State Controls Reactivity in Triplet Photocycloaddition. *J. Am. Chem. Soc.* **2005**, *127*, 4270–4285.